A Three-Dimensional Eutrophication Modeling in Tolo Harbour

K.W. Chau
Department of Civil & Structural Engineering, Hong Kong Polytechnic University, Hunghom, Kowloon, Hong Kong.

Abstract

Eutrophication phenomena may lead to less desirable water quality and usage of a water body in terms of water supply, fish maintenance, aesthetics and recreation. This paper delineates a real-time three-dimensional finite difference numerical model for eutrophication dynamics in coastal waters of Tolo Harbour, Hong Kong, employing the numerically generated, boundary-fitted, orthogonal curvilinear grid system as well as a grid "block" technique. The difficulties encountered, subtleties of the modeling as well as some principal kinetic parameters are described. Besides, the long-term time-series simulation results due to time-varying pollution sources in Tolo Harbour are presented.

Keywords

Three-dimensional model; environmental modeling; eutrophication phenomena; real-time simulation; boundary-fitted co-ordinates; Tolo Harbour

Introduction

In recent decades, with the rapid growth in economic development and population, a side effect is an increasing tendency of eutrophication phenomena in some water bodies. It is usually evidenced by the drastic increase in the severity and frequency of algae blooms, which are stimulated by the excessive input of nutrients into a water body. It may lead to less desirable water quality and usage of the water body in terms of water supply, fish maintenance, aesthetics and recreation, as well as are associated with problems such as bottom-water anoxia, decline in fisheries, and loss of submerged aquatic vegetation. Research was initially focussed on eutrophication modeling at seasonal steady-state conditions. Then time-varied modeling for a longer period in years was explored (Lung et al., 1993). In order to assess accurately the long-term recovery of an ecosystem through different possible management strategies, eutrophication modeling has been integrated with hydrodynamic models incorporating sediment layers (Cerco and Cole, 1993). Previously, owing to the limitation of computing resources, pollutant transport modeling was undertaken with several water quality parameters in depth-integrated two-dimensions or small number of parameters in three-dimensions. With the advances of computer technology, fluid flow and

interactions of various water quality variables in natural water bodies can be described fully in real-time.

Traditionally, many areas of coastal waters in Hong Kong received sewage directly from the urbanized catchments, as well as waste discharges from domestic, livestock and industrial sources via streams and stormwater runoffs. These discharges conveyed a heavy loading of nutrients entailed for the growth of phytoplankton, resulting in high eutrophic potential and deterioration of water quality. Tolo Harbour (Fig. 1) is an almost land-locked sea inlet with a narrow outlet in the South China Sea. It has an area of about 52km^2 and is approximately 16km from the Southwest at inner harbour to the Northeast at outer channel. The water depth varies from about 2m in the inner part to over 20m in the outer part of Tolo Channel and about 12m on average. The averaged diurnal tidal difference is about 0.97 m, mean high tide is 1.75 m and mean low tide is 0.78 m chart datum.

During the summer, the differences in surface and bottom water temperature and salinity, engendered by solar radiation and rainfall, result in density stratification within the water column (Chau and Jin, 1995). It enlarges the vertical gradient of pollutant concentration and weakens the vertical mixing. Bottom waters in Tolo Harbour exhibit serious dissolved oxygen (DO) depletion whilst the DO content remains adequate at the surface (EPDHK, 2000). In the winter, owing to increased turbulent mixing through the strong northeast monsoon and lower bottom sediment oxygen demand (SOD) exerted at a lower temperature, higher DO levels in the bottom waters are normally observed. In particular, the anoxic status in bottom waters during the summer cannot be simulated satisfactorily using a conventional depth-integrated model, rendering it necessary to develop a full model. This paper presents a rigorous three-dimensional (3D) numerical eutrophication model, integrating hydrodynamics with water quality and simultaneously incorporating SOD and nutrient releases from sediments. The objective of this study is to simulate time-varying water quality transport in a density stratified natural water body during the eutrophication process. The difficulties encountered, subtleties of the modeling as well as some principal kinetic parameters are delineated. Besides, the long-term time-series simulation results due to time-varying pollution sources in Tolo Harbour are presented.

Model Framework

Eutrophication modeling is used to simulate the balance of mass and energy within an ecosystem, in which a variety of physical, chemical, biochemical, and biological processes underlie the transport and interaction among the nutrients, phytoplankton, zooplankton, carbonaceous material, and DO in the aquatic environment (Orlob, 1983). The entire system is highly coupled since the energy and mass balances for each constituent are linked to one

another. In this model, a system of nine state variables are considered, namely, three organic parameters (carbonaceous biochemical oxygen demand (CBOD), nitrogen and phosphorus), four inorganic parameters (DO, NH_4-N, NO_2 + NO_3-N and PO_4-P), and two biological constituents (phytoplankton and zooplankton). It is developed, calibrated, and verified for Tolo Harbour, Hong Kong. Both organic nitrogen and organic phosphorus are divided into particulate and dissolved concentrations. NH_4-N, NO_2 + NO_3-N and PO_4-P are considered as the available nutrients taken up by phytoplankton. PO_4-P is also divided into particulate and dissolved concentrations, and its dissolved phase is available for phytoplankton uptake. The existing 10 years' field data during 1991-2000 in Tolo Harbour showed that silicate is plentiful and is excluded as a limiting nutrient. Moreover, local field data on hourly solar radiation intensity (I), water temperature (T), and salinity (S) are used.

Governing equations

The algorithm is designed to have an integrated hydrodynamic and water quality model having a common computational grid and time steps. For all variables in the following discussions, subscript "k" means the value in the k^{th} layer, subscript "u" and "l" mean the value in the upper layer and lower layer, respectively. Notation $X_{y,20}$ designates the value of X_y at temperature 20°C, and θ is the corresponding temperature correction coefficient.

Under the boundary-fitted orthogonal curvilinear co-ordinate system, the followings show differential transport equations for layer-averaged concentration of a state variable:

$$\frac{\partial(h_k\varphi_k)}{\partial t}+\frac{1}{g_{11}g_{22}}\left\{\frac{\partial}{\partial\xi}\left[g_{22}h_k\left(u_k^*\varphi_k-\frac{\Gamma_{\xi,k}}{g_{11}}\frac{\varphi_k}{\partial\xi}\right)\right]+\frac{\partial}{\partial\eta}\left[g_{11}h_k\left(v_k^*\varphi_k-\frac{\Gamma_{\eta,k}}{g_{22}}\frac{\varphi_k}{\partial\eta}\right)\right]\right\}=\Phi_{\varphi,k} \quad (1)$$

$$\Phi_{\varphi,k}=w_k\varphi_k+Flux_{u,\varphi}-Flux_{l,\varphi}+S_{\varphi,k} \quad (2)$$

where u_k^* and v_k^* = layer-averaged velocity components in ξ-η orthogonal curvilinear co-ordinates; h_k = water depth; φ_k = layer-averaged concentration of the state variable, representing DO, phytoplankton, or others; $\Gamma_{\xi,\kappa}$ and $\Gamma_{\eta,\kappa}$ = longitudinal and transverse dispersive coefficients, respectively: g_{11} and g_{22} = co-ordinate transformation coefficients between Cartesian and orthogonal curvilinear co-ordinates (ξ,η); $S_{\varphi,k}$ = reaction kinetics, settling, sediment release, sources, or sinks and w_k = vertical velocity at the layer interface.

$Flux_{k,\varphi}$ is expressed, considering density stratification, as:

$$Flux_{k,\varphi} = \left(\Gamma_m \frac{\partial \varphi}{\partial z} \right)_{z=Z_0} , \ \Gamma_m = \Gamma_{m0} (1 + \beta_C \, Ri \,)^{\alpha_C} \tag{3}$$

in which Γ_m = vertical flux diffusive coefficient, Γ_{m0} = values of Γ_m for the case without density stratification, β_C (=10/3) and α_C (=-1.5) are the empirical coefficients (Rodi 1980). Ri is a gradient Richardson number at the layer interface and is calculated by:

$$\mathrm{Ri} = -\frac{g}{\rho} \frac{\frac{\partial \rho}{\partial z}}{(\frac{\partial u}{\partial z})^2} \approx \frac{\rho_l - \rho_u}{\rho} \frac{g\delta}{[(u_u^* - u_l^*)^2 + (v_u^* - v_l^*)^2]} \tag{4}$$

in which ρ_u and ρ_l = density of water in the upper and the lower layer, respectively, ρ = averaged density of water column, g = acceleration due to gravity, δ = mixing layer thickness at the interface. The density of water is computed on the basis of the continuous temperature and salinity measurement data.

Settlement causes decrease in quantities of water quality variables. The rate of algal growth depends upon available nutrients, water temperature, solar radiation, zooplankton grazing, tidal flushing, etc. Organic nitrogen undergoes a bacterial decomposition whose end product is ammonia (NH_4-N). Organic phosphorus is converted to PO_4-P by mineralization. Ammonia nitrogen, in the presence of nitrifying bacteria and oxygen, is converted to NO_3-N. Denitrification occurs under anaerobic conditions and CBOD decreases due to stabilization. Both NH_4 and NO_2 + NO_3 are available for algae uptake, however, the preferred form is NH_4-N for physiological reasons. Expressions are written to represent all these processes. For instance, the ammonia preference is described by a factor f_{pref}:

$$f_{pref,k} = \frac{NH_{4,k}}{K_{mNN} + NO_{23,k}} \left(\frac{NO_{23,k}}{K_{mNN} + NH_{4,k}} + \frac{K_{mNN}}{NH_{4,k} + NO_{23,k}} \right) \tag{5}$$

The production of DO is a by-product of photosynthetic carbon fixation. An additional source of oxygen from algal growth occurs when the available ammonia nutrient source is exhausted and the phytoplankton begins to utilize the available nitrate. For nitrate uptake, the initial step is a reduction to ammonia, which produces oxygen. DO also increases by atmospheric re-aeration (k_a, day^{-1}) because of the deviation from the saturation concentration DO^s (mgO_2/l). The re-aeration rate in natural waters depends on internal mixing and turbulence due to velocity gradients and fluctuation, temperature, wind mixing, waterfalls, dams, rapids, surface films, etc. and is expressed as follows:

$$k_a = k_{a,20}\theta^{T-20}\ , \quad \theta = 1.005 \sim 1.030 \approx 1.024 \tag{6}$$

$$k_{a,20} = \begin{cases} \dfrac{3.9V^{0.5}}{h^{1.5}}\ , & \text{when } W < 6.0\text{m/s;} \\ \dfrac{3.9V^{0.5}}{h^{1.5}} + \dfrac{0.728W^{0.5} - 0.317W + 0.0372W^2}{h}\ , & \text{when } W \geq 6.0\text{m/s} \end{cases} \tag{7}$$

$$\ln DO^s = -139.3441 + \frac{1.5757\times10^5}{T+273.15} - \frac{6.6423\times10^7}{(T+273.15)^2} + \frac{1.2438\times10^{10}}{(T+273.15)^3} - \frac{8.6219\times10^{11}}{(T+273.15)^4} - S\left[1.7674\times10^{-2} - \frac{1.0754\times10}{T+273.15} + \frac{2.1407\times10^3}{(T+273.15)^2}\right] \tag{8}$$

where V is velocity of flow in m/s; W is wind speed in m/s at 10m above water surface (it will be taken into account when wind speed W≥6m/s); T (°C) and S (ppt) are the relevant water temperature and salinity. A minimum value of 1.6/h is imposed on $k_{a,20}$. Moreover, there is an adsorption-desorption interaction between dissolved inorganic phosphorus and suspended particulate matter in the water column. The subsequent settling of the suspended solids together with the sorbed inorganic phosphorus can act as a significant loss mechanism in the water column and is a source of phosphorus to the sediment.

Phytoplankton dynamics and nutrient kinetics

Table 1 lists typical kinetic parameters used in the 3D eutrophication model, which are calibrated with the field data for the scenario in Tolo Harbour or come from the literature (Ambrose et al., 1988; Lee et al., 1991b; Thomann and Mueller, 1987). The growth and proliferation of phytoplankton is a result of the utilization and conversion of inorganic nutrients into organic plant material through photosynthesis, μ_A depends on three principal components: (a) Temperature — T, (b) solar radiation — I, (c) nutrients — N_{nutri}. Multiplicative effects are assumed, i.e., $\mu_A = f(T, I, N_{nutri}) = g(T)g(I)g(N_{nutri})$.

The relationship with temperature is as follows:

$$g(T)_k = \mu_{A,k}^{\max} = \mu_{A,20}^{\max}\theta^{T_k-20} \tag{9}$$

where $\mu_{A,20}^{\max}$ = maximum growth rate of phytoplankton at 20°C under optimal light and nutrient

conditions in the k^{th}-layer.

In this model, the light-limitation function of Steele and Baird (Thomann and Mueller, 1987) is used. g(I) over a given water depth of layer (h_k) is approximately integrated as:

$$g(I)_k = \frac{1}{h_k}\int_{h_u}^{h_u+h_k} \frac{I}{I_s} e^{(1-\frac{I}{I_s})} dz = \frac{2.718}{\gamma_k h_k}[e^{-\alpha_2} - e^{-\alpha_1}]$$

$$\alpha_2 = \alpha_1 e^{-\gamma_k h_k}, \alpha_0 = \frac{I_0}{I_s}, \ \alpha_1 = \alpha_0 e^{-\gamma_u h_u} \quad (10)$$

$$\frac{dI}{dz} = -\gamma_k I, \quad I = I_0 @ z = 0, \text{ and z - axis is upward vertically}$$

where I, I_0 and I_s = light intensity at depth z, incoming solar radiation intensity just below the surface and saturating light intensity (the optimum light intensity at which the relative photosynthesis is a maximum), respectively; and γ_κ = overall extinction coefficient in m^{-1}. For Tolo Harbour, Lee et al. (1991a) have suggested the following formula:

$$\gamma_k = 0.24 - 0.0057A_k + 0.145A_k^{1/2} \quad (11)$$

in which A_k (μg Chl-a/L) is the averaged concentration of Chl-a. Phytoplankton may adjust its chlorophyll composition to adapt to the changes in solar radiation. Therefore, I_s is determined to be the weighted average of the light intensity for the previous three days as follows: $I_s = 0.7I_1 + 0.2I_2 + 0.1I_3$, where I_i=0.5×[daily average visible light intensity beneath the surface] i days earlier (Lee et al., 1991b). The annual average of daily solar radiation intensity in Tolo Harbour is about 300 ly/day. Hourly I_0, issued by the Royal Observatory of Hong Kong, is used in the modeling.

The minimum value of nutrient limitations computed by Michaelis-Menten-type expression (Thomann and Mueller, 1987) is chosen for $g(N_{nutri})$. Thus, the full expression for layer-averaged phytoplankton growth rate is expressed as:

$$\mu_{A,k} = \mu_{A,k}^{\max} g(I)_k \min\left\{\frac{NH_{4,k} + NO_{23,k}}{K_{mNN} + NH_{4,k} + NO_{23,k}}, \frac{PO_{4,k} \cdot f_{DPO_4}}{K_{mNP} + PO_{4,k} \cdot f_{DPO_4}}\right\} \quad (12)$$

in which $NH_{4,k}$ (μgN/L), $NO_{23,k}$ (μgN/L), and $PO_{4,k}$ (μgP/L) = concentrations of NH_4-N, NO_2 + NO_3-N and PO_4-P in kth layer, respectively; K_{mNN} (μgN/L) and K_{mNP} (μgP/L) = Michaelis

constants for nitrogen and phosphorus uptake by algae, respectively.

Depending on the past history of the algal cells, the CCHL ratio (mg C/mg Chl-a) is affected by light intensity, temperature, and nutrient availability. The following expression is used here:

$$CCHL = \frac{\alpha I_s}{2.718 \mu_{A,k}^{\max}} \tag{13}$$

where $\alpha \cong 6.0$ mg C/mg Chl-a·ly from Lee et al.'s (1991b) laboratory results. The averaged value of CCHL is 112.5 mg C/mg Chl-a.

A saturating recycle equation is used for hydrolysis and bacterial decomposition of organic nitrogen to ammonia (k_{34}) and the mineralization of organic phosphorus to inorganic phosphorus (k_{67}):

$$k_{34} = k_{34,20}\theta^{T_k-20}\frac{A_k}{K_{mpc}+A_k}, \quad k_{67} = k_{67,20}\theta^{T_k-20}\frac{A_k}{K_{mpc}+A_k} \tag{14}$$

This form of expression is a compromise between the conventional first-order temperature-corrected mechanism and a second-order recycle mechanism with the recycle rate being directly proportional to the amount of phytoplankton biomass. It approaches second order dependency at low phytoplankton concentrations ($A<<K_{mpc}$), where K_{mpc} is the half-saturation constant for recycle, and approaches first order recycle when the phytoplankton greatly exceeds the half-saturation constant. This mechanism slows the recycle rate if the algal population is small but not permit the rate to increase continuously as phytoplankton increases since at higher population levels other factors are limiting the recycle kinetics.

The following processes, namely, nitrification (k_N) of NH_4 to NO_3 via NO_2-N, denitrification (k_{55}) of NO_3-N and deoxygenation (k_C) of CBOD, are considered temperature and oxygen dependent:

$$k_N = k_{N,20}\theta^{T_k-20}\frac{DO_k}{K_{NIT}+DO_k}, \; k_{55} = k_{55,20}\theta^{T_k-20}\frac{K_{NO}}{K_{NO}+DO_k}, \; k_C = k_{C,20}\theta^{T_k-20}\frac{DO_k}{K_{BOD}+DO_k} \tag{15}$$

where DO_k (mg O_2/L) = concentration of DO; K_{NIT} and K_{BOD} (mg O_2/L) = half-saturation DO constants for oxygen limitation of nitrification and of organic carbon stabilization; K_{NO} (mg O_2/L) = half-maximum DO constant for denitrification.

Primary production by phytoplankton in surface waters is a major source of labile organic carbon to coastal sediment. Particles from the euphotic zone sink to the sediment-water interface, where benthic organisms rapidly degrade the labile organic compounds present in the settled materials (Di Toro et el., 1990). In this model, sediment algal carbon is expressed as follows:

$$\frac{dC_{sedi}}{dt} = \alpha_{sediCA} w_{SA} A_l - \frac{v_{sedi}}{h_{sedi}} C_{sedi} - k_{Csedi} C_{sedi} \tag{16}$$

where C_{sedi} (g C/m^2) = sediment algal carbon; α_{sediCA} (g C/g Chl-a) = sediment algal carbon per unit algal mass settled; v_{sedi} (m/day) = sediment accumulation rate; h_{sedi} (m) = thickness of the sediment layer; k_{Csedi} (day^{-1}) = oxidation rate of sediment algal carbon. In this model, v_{sedi}/h_{sedi} = 0.001 day^{-1}, $k_{Csedi} = 0.15(1.047)^{T_l - 20}$ day^{-1}. Hence, SOD includes oxidation of sediment algal carbon (SOD_C) and other processes (SOD_0):

$$\begin{aligned} &SOD = SOD_C + SOD_0 \\ &SOD_C = 32 k_{Csedi} C_{sedi}/12 \ , \quad \mathrm{SOD}_0 = SOD_{0,20}(1.074)^{T_l - 20} \end{aligned} \tag{17}$$

An in-situ field study shows that $SOD_{0,20}$ in Tolo Harbour is between 0.47 and 1.24 g O_2/m^2/day and about 0.88 g O_2/m^2/day on average. Apart from the external sources of nutrients, the impact of sediment nutrient releases is significant which results in continuing eutrophication problems even after point sources are substantially reduced through control measures. Such releases occur as a result of a gradient in nutrient concentration between the overlying water and the nutrient in the interstitial water of the sediment. Table 2 shows the sediment releases of nutrients from in-situ analysis on nearly 80 samples at five different locations in Tolo Harbour.

Numerical method

Tidal elevation at the open boundary is calculated from a harmonic analysis of a long series of tidal observations at a nearby tide gauge – Kau Lau Wan using 42 tidal constituents. The concentrations of all water quality variables at the open boundary are specified with measured data when water flows into the water body of interest, and the normal gradients of the concentrations are simply taken as zero when water flows out from the water body. The normal gradients for all water quality variables at bank boundary are specified as zero. The initial conditions are obtained by interpolating the corresponding boundary values at the starting time. It is found that the lead time for reliable results is very short.

In the model, a staggered grid (Arakawa C) system is adopted, in which the nodes for water quality state variables and water surface elevation do not coincide with that for water velocities. The differential equations governing water quality processes are discretized by control-volume formulation. The computational domain is divided into non-overlapping control volumes surrounding every grid point. The differential equation is integrated over each control volume with piecewise profiles expressing the variation of the variable between the grid points. The discretized equation expresses the conservation principle for the variable in the finite control volume. After integrating Eq. 1 in the control volume, an equation set of linearized discretized equation for each state variable can be obtained, which can be solved by tri-diagonal matrix algorithm with alternating direction iteration. The procedure of the solution in one time step calculates the hydrodynaimc variables first and then the equations for phytoplankton, zooplankton, organic nitrogen, NH_4-N, NO_2+NO_3-N, organic phosphorus, PO_4-P, CBOD and DO are solved in sequence. The procedure is carried out step-by-step and the temporal hydrodynamic and water quality parameters are then acquired.

Environmental Modeling in Tolo Harbour

Tolo Harbour catchment in Hong Kong was formerly a rural area. It has been increasingly developed since the mid-1960s as a source of potable water and the site of two major new towns, Shatin and Tai Po with populations of nearly 700,000 and 300,000, respectively. The Tolo waters receive sewage directly from the urbanized catchments, as well as waste discharges from domestic, livestock, and industrial sources via streams, etc. The water quality in recent years has declined dramatically (EPDHK, 2000), and it can be regarded as highly eutrophic, exhibiting high algal growth. Tolo Harbour was declared as the first Water Control Zone in Hong Kong and statutory water quality objectives, specifying the target concentrations of different parameters at different locations of Tolo Harbour, were established in 1982. In the past decades, a number of engineers and scientists have carried out investigations in Tolo Harbour with a view to predicting and recording the effects of development on levels of pollution in the water (Chau and Sin, 1992; Chau et al., 1996; Hodgkiss and Chan, 1983; Lee et al., 1991a,b; Sin and Chau, 1992). It was estimated that the average retention time in the inner harbour is about 35 days (Hodgkiss and Chan, 1983).

Owing to density stratification in Tolo waters, it is appropriate to describe the water quality dynamics using a 3D model. This model was calibrated and verified with the long-term time-series field data in Tolo Harbour, Hong Kong. The results show that the flow directions in the surface and the bottom layer in the harbour may be non-uniform, especially when the current is not too swift. The computed velocities in most of the harbour, especially in the outer area, i.e., in

Tolo Channel, have a prevailing direction along the channel, and its transverse component is very small relative to its longitudinal counterpart. In the side coves, however, flow directions in the surface layer are generally different from those in the bottom layer. The pollution sources entering the harbour consist of those from five main tributaries and those from outfalls of two sewage treatment plants at Shatin and Tai Po, which are time-varying and are taken as point-sources.

Tolo Harbour is very irregular on the lateral topography and includes some small side coves. To adapt the complicated boundaries of the water body, a boundary-fitted orthogonal curvilinear grid system with a total of 1580 grid cells is employed. Longitudinal grid size is about 110-710 m and transverse size about 60-530 m. Maximum ratio of the longitudinal to the transverse grid size is nearly 8.5. It is generated numerically by solving two elliptical equations (Thompson et al., 1985). In addition, a grid "block" technique (Chau and Jiang, 2001 & 2002) is introduced to overcome the computational difficulty caused by the unsteady fluctuation of water surface level.

Whilst the measured data during 1995-1996 are used to calibrate the kinetic parameters in the model, the model is verified by the data during 1998-1999. The time step of the model run is set to 5 minutes. Fig. 2 shows the long-term time-series results computed and measured at TM4 during 1998-1999 in the surface layer and bottom layer, respectively. The major ticks on the time abscissa in Fig. 2 designate year and the minor ticks indicate month. The oscillation on model predictions for Chl-a and other variables reflects the complexity of ecological processes. It may be caused by variations in light intensity, pollutant loadings, tidal flow, density stratification, water temperature and salinity, etc. The light intensity affects the algal growth and photosynthesis. The nutrient concentrations are closely linked to their loadings, their kinetics, algae and zooplankton dynamics and so on. The mixing and transport of both momentum and water quality are governed by the tidal flow and density stratification. A reasonable examination of the numerical model appeared to be that its predictions should agree closely with the central trend of the observations. As shown in Fig. 2, the computational results by the present 3D model mimic the measured data in Tolo Harbour, i.e., the model could represent reasonably the algal growth dynamics and water quality processes, including layer-averaged Chl-a, DO, $CBOD_5$, organic nitrogen, NH_4-N, NO_2 + NO_3-N, organic phosphorus, and PO_4-P concentrations, in different layers.

When the surface water in the harbour is generally well oxygenated, serious oxygen depletion problem often occurs during the summer and extremely low DO levels, below 5% saturation, are recorded occasionally throughout the whole bottom waters. These are caused by the high oxygen demand from the decay of organic matter in the bottom sediment at higher summer temperatures. The respiration of benthos further uses up the oxygen in the bottom water. At the same time, the weak turbulent mixing together with the steep temperature and salinity stratification in the water column, showing an obvious lighter upper water layer and a definite mesolimnion, prevents

vertical mixing and replenishment of oxygen from the well aerated surface water to the bottom. As a result, the bottom water becomes anoxic and a steep vertical stratification in DO is formed. In the winter, higher DO levels in the bottom waters are generally recorded. The computational results show correctly the stratification tendency in all the water quality state variables, serious oxygen depletion and anoxic condition in the bottom layers when the surface waters may still be well oxygenated during the summer. Moreover, during the winter, the results reflect the vertically uniform concentration of water quality.

It is found that the water quality processes in different layers in Tolo waters are similar except for their differences in magnitude. In general, water quality in the Tolo Channel is better than that in the inner harbour. The water in the inner harbour has been seriously polluted due to substantial pollution loads and poorly tidal flushing. During January and February, the water temperature is low and the solar radiation is weak, low chlorophyll-a concentration and saturated DO are the features of the water body. During the spring and the early summer, starting from March, water temperature rises and solar radiation intensifies, chlorophyll-a concentrations can attain their annual maximum and nutrients are rapidly depleted by the algal bloom. Ammonia and orthophosphate concentrations in the bottom layer, due to less uptake by the phytoplankton and the sediment releases, are higher than those in the surface layer. Meanwhile, the DO can maintain a super-saturated period due to photosynthesis and then rapidly decrease because of the activity of settled algal carbon as SOD and reaches its annual minimum near June. The bottom water anoxia may occur, especially in the inner harbour, and the anoxic condition may retain for a prolonged period. From later summer till December, the lower chlorophyll-a concentration is maintained and the DO is restored gradually to its saturated state. Nutrients also increase gradually due to less utilization by algae during that period. Thus one annual cycle is completed.

Moreover, the simulation shows that zooplankton affects algal populations in Tolo waters. The zooplankton concentration is very low, nearly zero, from January to May, rises from June, attains its annual maximum between September and October and then reduces to nearly zero again by the end of December. The variation of zooplankton is rational. The algal concentration in both layers in Tolo Harbour, especially in the inner harbour and in the buffer zone, almost never reached very low values. The predicted zooplankton biomass dynamics are different from the algae and similar to the water temperature. The zooplankton concentration in the bottom layer is lower than that in the surface layer accordingly.

Conclusions

A real-time 3D numerical model for eutrophication, based upon the numerically generated, boundary-fitted orthogonal curvilinear grid system with a grid block technique and integrated

with the prediction of a hydrodynaimc variables simultaneously, has been implemented. The model simulates the transport and transformation of nine water quality constituents associated with eutrophication in the waters, including Chl-a, DO, CBOD, organic nitrogen, NH_4-N, NO_2 + NO_3-N, organic phosphorus, PO_4-P, and zooplankton. The comparison of computational results with measured data available in Tolo Harbour demonstrates its capability to mimic the algal growth dynamics and water quality processes reasonably. Thus the model can be used to predict the eutrophication potentials and the effectiveness of possible management solution strategies.

Acknowledgement

This project was supported by a grant from the Research Grant Committee of the University Grant Council of Hong Kong.

References

Ambrose, RB, Wool, TA, Connolly, JP, and Schanz, RW (1988). *WASP4, a Hydrodynamic and Water Quality Model — Model Theory, User's Manual, and Programmer's Guide,* US Environmental Protection Agency Report, EPA/600/3-87/039.

Cerco, CF, and Cole, T (1993). "Three-Dimensional Eutrophication Model of Chesapeake Bay," *Journal of Environmental Engineering, ASCE,* Vol 119(6), pp 1006-1025

Chau, KW, and Jiang, YW (2001). "3D Numerical Model for Pearl River Estuary," *Journal of Hydraulic Engineering, ASCE*, Vol 127(1), pp 72-82.

Chau, KW, and Jiang, YW (2002). "Three-Dimensional Pollutant Transport Model for the Pearl River Estuary," *Water Research*, Vol 36(8), pp 2029-2039.

Chau, KW, and Jin, HS (1995). "Numerical Solution of Two-Layered, Two-Dimensional Tidal Flow in Boundary-Fitted Orthogonal Curvilinear Coordinate System," *International Journal for Numerical Methods in Fluids,* Vol 21(11), pp 1087-1107.

Chau, KW, Jin, HS and Sin, YS (1996). "A Finite Difference Model of 2-D Tidal Flow in Tolo Harbour, Hong Kong," *Applied Mathematical Modelling*, Vol 20(4), pp. 321-328.

Chau, KW, and Sin, YS (1992). "Correlation of Water Quality Parameters in Tolo Harbour, Hong Kong," *Water Science and Technology*, Vol 26(9-11), pp. 2555-2558.

Di Toro, DM, Paquin, PR, Subburamu, K, and Gruber, DA (1990). "Sediment Oxygen Demand Model: Methane and Ammonia Oxidation," *Journal of Environmental Engineering, ASCE,* Vol 116(5), pp 945-986.

EPDHK (2000). *Marine Water Quality in Hong Kong:Results from the EPD Marine Water Quality Monitoring Programme for 1999,* Environmental Protection Department, Hong Kong Government, EP/TR 3/00.

Hodgkiss, IJ, and Chan, BSS (1983). "Pollution Studies on Tolo Harbour, Hong Kong," *Marine*

Environmental Research, Vol 10, pp 1-44.

Lee, JHW, Wu, RSS, and Cheung, YK (1991a). "Dissolved Oxygen Variations in Marine Fish Culture Zone," *Journal of Environmental Engineering, ASCE,* Vol 117(6), pp 799-815.

Lee, JHW, Wu, RSS, Cheung, YK, and Wong, PPS (1991b). "Forecasting of Dissolved Oxygen in Marine Fish Culture Zone," *Journal of Environmental Engineering, ASCE,* Vol 117(6), pp 816-833.

Lung, W., Martin, JL, and McCutcheon, SC (1993). "Eutrophication Analysis of Embayments in Prince William Sound, Alaska," *Journal of Environmental Engineering, ASCE,* Vol 119(5), pp 811-824.

Orlob, GT (1983). *Mathematical Modeling of Water Quality,* Wiley-Interscience, New York, N. Y.

Rodi, W (1980). *Turbulence Models and Their Application in Hydraulics, State-of-the-art,* IAHR Publication, DELFT, The Netherlands.

Sin, YS, and Chau, KW (1992). "Eutrophication Studies on Tolo Harbour, Hong Kong," *Water Science and Technology,* Vol 26(9-11), pp 2551-2554.

Thomann, RV, and Mueller, JA (1987). *Principles of Surface Water Quality Modeling and Control,* Harper & Row, Publishers, Inc., New York, N. Y.

Thompson, JF, Warsi, ZUA, and Mastin, CW (1985). *Numerical Grid Generation*, Elsevier Science Publishing Co., Inc., New York, N. Y.

Yih, CS (1980). *Stratified Flows*, Academic Press.

Table 1. Typical kinetic parameters used in the eutrophication model

Parameters	Description	Value (and θ)
μ_A^{max}	Maximum phytoplankton growth rate	2.10 (1.066)
K_{mNN}	Half-saturation constant for nitrogen uptake	15.0
K_{mNP}	Half-saturation constant for phosphorus uptake	1.50
r_A	Endogenous respiration rate of phytoplankton	0.05 (1.08)
M_A	Nonpredatory mortality rate of phytoplankton	0.10
C_g	Grazing (filtering) rate of zooplankton	0.30 (1.066)
r_Z	Endogenous respiration rate of zooplankton	0.02 (1.045)
M_Z	Mortality rate of zooplankton	0.10
α_{12}	Assimilated carbon per unit algae mass ingested (average CCHL)	112.5
α_2	Zooplankton assimilation efficiency	0.6
K_Z	Half-maximum-efficiency food level for zooplankton filtering	12.0
k_{34}	Conversion efficiency of organic nitrogen to ammonia nitrogen	0.05 (1.08)
α_{13}	Stoichiometric ratio of cell nitrogen to algae chlorophyll-a	10.0
α_{23}	Stoichiometric ratio of cell nitrogen to zooplankton carbon	α_{13}/CCHL
k_N	Nitrification rate of ammonia to nitrate via nitrite nitrogen	0.05 (1.08)
k_{55}	Denitrification rate	0.09 (1.045)
k_{67}	Conversion efficiency of organic phosphorus to inorganic one	0.03 (1.08)
α_{16}	Stoichiometric ratio of phosphorus to algae chlorophyll-a	1.00
α_{26}	Stoichiometric ratio of phosphorus to zooplankton carbon	α_{16}/CCHL
k_c	Deoxygenation or decay rate of carbonaceous BOD	0.23 (1.047)
BOD_{u-5}	Ratio of the ultimate to 5-day carbonaceous BOD	1.54
α_{18}	Stoichiometric ratio of phytoplankton to organic carbon	CCHL
α_{28}	Stoichiometric ratio of zooplankton to organic carbon	1.00
α_{ON}	Oxygen to nitrogen ratio	2.28
α_{19}	Stoichiometric ratio of phytoplankton to oxygen	2.67CCHL
K_{mpc}	Half saturation constant for phytoplankton affects mineralization	10.0
K_{NIT}	Half saturation DO constant for oxygen limitation of nitrification	2.0
K_{NO}	Half-max. DO constant for oxygen limitation of denitrification	0.1
K_{BOD}	Half saturation DO constant for CBOD deoxygenation.	0.5
w_{SA}	Settling rate of phytoplankton	1.10
w_{SN}	Settling rate of particulate organic nitrogen	0.30

Table 2. Sediment releases of nutrients from in-situ analysis

Parameters	Range of value	Unit
Organic nitrogen	6 - 40	mg $N/m^2/day$
NH_4-N	18 - 205	mg $N/m^2/day$
NO_2+NO_3-N	-4.43 - 9.16	mg $N/m^2/day$
Organic phosphorus	0.17 - 1.61	mg $P/m^2/day$
PO_4-P	1.45 - 8.90	mg $P/m^2/day$

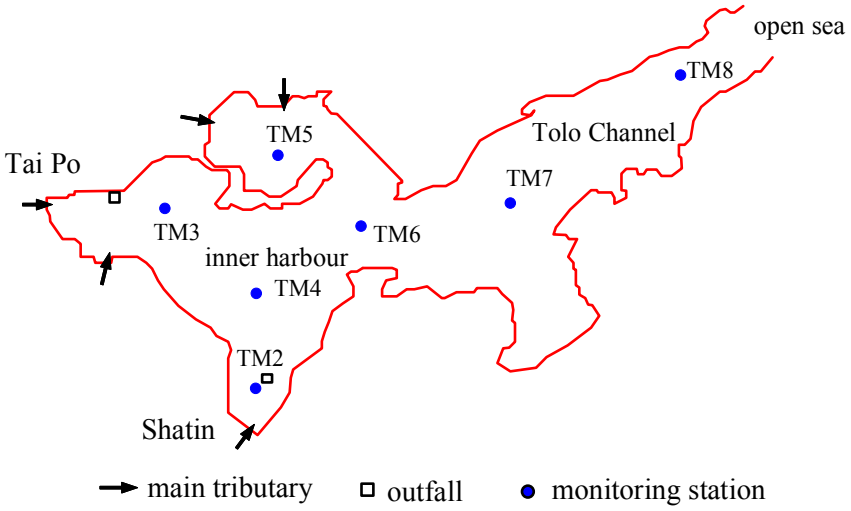

Fig.1 The Tolo Harbour, Hong Kong

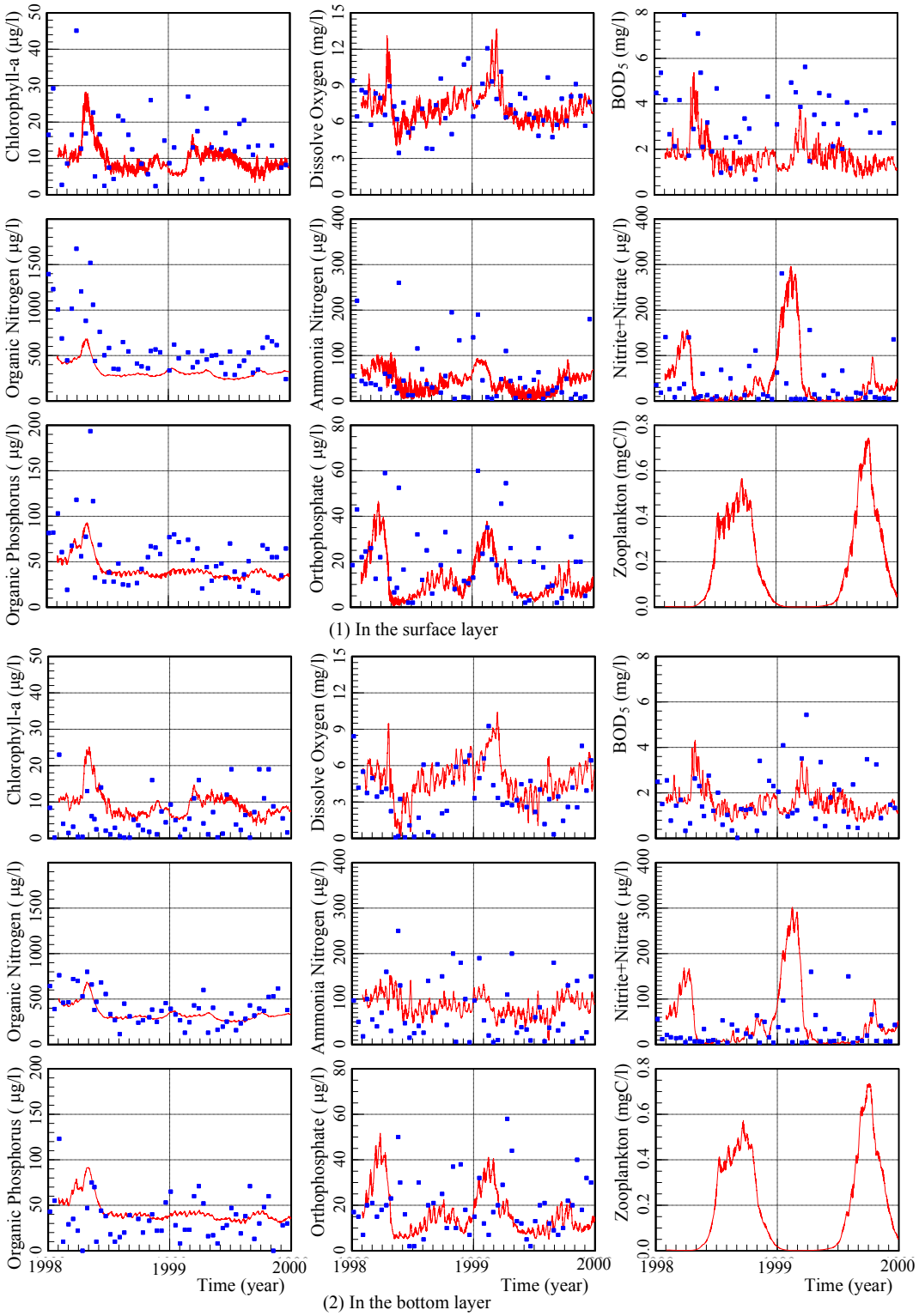

Fig.2 Long-term time-series comparisons of results computed and measured at TM4 in surface layer and bottom layer respectively for Tolo Harbour, Hong Kong, during 1998~1999 (— computed, ▪ measured)